# Stability of Sliding Mode ILC Design for a Class of Nonlinear Systems With Unknown Control Input Delay

Xiaoyu Zhang, *Senior Member, IEEE*, and Richard W. Longman, *Member, IEEE*

***Abstract*— This article studied the stability and convergence of a robust iterative learning control (ILC) design for a class of nonlinear systems with unknown control input delay. First, the iterative integral sliding mode (IISM) design was proposed, which comprised iterative actions. The iterative action made the convergence of the tracking error under the ideal sliding mode. Then, a suitable iterative update law was provided for the IISM-based robust ILC controller. The controller had the capability of both minimizing the steady tracking error and suppressing the unrepeatable disturbance. Using the controller, the closed-loop system stability was analyzed, and the stability conditions were given. Consequently, the sliding mode convergence in the iteration domain was proved by a composite energy function (CEF). In addition, by analyzing the influence of affection on the tracking error, several measures were taken to solve the chattering problem of the sliding mode control. Finally, a one-link robotic manipulator and a vertical three-tank system were used to verify the control design. The application simulations validated the performance of the proposed sliding mode iterative learning control (SMILC) design, which achieved the stability of the nonlinear system and overcame the control input time delay.**

***Index Terms*— Adaptive, iterative learning control (ILC), nonlinear systems, robust, sliding mode.**

## I. Introduction

THE iterative learning control (ILC) method is an excellent control design for repeating control tasks. In recent years, it has been widely used in various fields, such as manipulators, robotics, chemical processes, and accurate disk control, due to its advantages, especially less requirement of prior knowledge about the controlled plant. Its steady error can reach nanolevel, which shows that it is a strong tool to resolve the problem of perfect tracking [1].

In addition to discrete systems, ILC research work has been extended to linear and nonlinear systems [2]. For continuous-time LTI and LTV systems, different designs were proposed in both the time domain and the frequency domain, and the stability and convergence analysis were analyzed in both domains. It provided perfect tracking performance on linear systems. However, ILC cannot provide perfect tracking performance in every situation. If there are noise and nonrepetitive disturbances, observers, robust filtering, and combined controller design are always needed. The iterative learning feature of ILC encourages the addition of more synthesis methods to the ILC system design, such as advanced filtering, signal processing, and other control methods. Longman [3] discussed the relevance of many of this type of techniques. For nonlinear systems, research can be divided into two categories. The first category focused on the systems for affine control input, such as the studies in the literature [4]–[8]. The affine nonlinear systems use a key assumption that the nonlinear dynamic is smooth and usually expressed as a global Lipschitz constraint. The in-depth studies on the nonlinear ILC can be found, including robust performance, transient learning, initial variations, repeating disturbance, and model uncertainty [4]–[6]. Another category of research on nonlinear ILC is aimed at nonaffine systems in control input [9]. Meanwhile, scholars also conducted in-depth studies on ILC designs for discrete-time nonlinear systems. Discrete-time models of nonlinear systems may not be easy to obtain. However, compared to continuous-time counterparts, discrete-time models always obtain simpler application control algorithm. This applies to both affine systems and nonaffine systems [10]–[14].

The development of control theoretical research is so extensive that many individual articles often discuss special topics. These have led to numerous topics related to ILC. In addition to controller structures, update laws, and convergence analysis, the popular papers in control theory or engineering fields have also attracted a lot of attention such as "robustness," "optimal and optimization," "event-triggered control [15]," and "quantized feedback [16]." Especially, the topics of robustness, adaptability, and compensation have advanced the development of the ILC algorithm [17]. For example, the $H_\infty$ framework is used to resolve ILC problems. $H_\infty$ performance index and the convergence along the iteration have been analyzed. The linear matrix inequality (LMI) technique was also adopted in many convergence analyses [18].

Although many ILC design approaches have been developed, an important topic related to ILC, i.e., the control problem concerning time-delay systems, still requires in-depth

Manuscript received 30 October 2019; revised 10 September 2020 and 6 January 2021; accepted 27 January 2021. Date of publication 19 February 2021; date of current version 2 September 2022. This work was supported in part by the National Natural Science Foundation of China under Grant 61304024 and in part by the China Scholarship Fund under Grant 201708130227. *(Corresponding author: Xiaoyu Zhang.)*

Xiaoyu Zhang is with the School of Electronic and Information Engineering, North China Institute of Science and Technology, Beijing 101601, China (e-mail: xyzhang@ieee.org).

Richard W. Longman is with the Department of Mechanical Engineering, Columbia University, New York, NY 10025 USA (e-mail: rwl4@columbia.edu).

Color versions of one or more figures in this article are available at https://doi.org/10.1109/TNNLS.2021.3056680.

Digital Object Identifier 10.1109/TNNLS.2021.3056680

study. Delays are inherent in many applications, such as batch processes and networked controlled robots and vehicles. Many actuators and sensors usually introduce delay, which degrades the performance of a control system. Many delay-related studies were only conducted within the framework of classical ILC. Meng *et al.* [19], [20] presented a PD-type ILC for uncertain linear systems with state time delay, proved the convergence by Lyapunov-like technique, and achieved the robust ILC algorithm. Wang *et al.* [21] adopted the T-S fuzzy model to establish an adaptive ILC control scheme for the state time delay of the linear systems. Liu *et al.* [22] proposed an ILC control method based on the internal model control (IMC) structure for batch processes of a linear transfer function model, including uncertainties and time delay. Some scholars discussed some special systems with time delay. For instance, Dai *et al.* [23] investigated the P-type ILC schemes of a system described by parabolic partial difference equations with delay. Lan and Zhou [24], [25] and Lazarevic *et al.* [26] considered fractional-order linear time-delay systems.

The systems with state time delay have been investigated in some studies. For example, Chen and Zhang [27] extended a CEF-based adaptive ILC strategy for nonlinear time-varying systems with state delays. It can deal with time-varying delays with a common adaptive learning law in the iteration domain. Wang *et al.* [28] proposed a robust ILC scheme for batch processes with uncertain perturbations and state time-varying delay and tried to convert it into a robust control problem of the uncertain 2-D system. Wei *et al.* [29] proposed an adaptive ILC scheme for a class of nonlinear systems with unknown time-varying state delay and introduced a boundary layer function to construct the error variable that relaxed the identical initial condition. The integral Lyapunov function and the appropriate Lyapunov–Krasovskii function were used to analyze the stability and convergence. Part of the research focused on the robust ILC scheme for nonlinear systems. For example, Shen [30] proposed an ILC algorithm for nonlinear systems with dead-zone input and state time delay with measurement noise. The nonlinear dynamics in systems required conditions similar to the Lipschitz continuity, and the update law was obtained through optimization. Ma [31] adopted the likely conditions and proposed an ILC design for nonlinear systems with multiple state delays. Meanwhile, the external disturbances and output measurement noises were also discussed. Bu *et al.* [32] proposed a robust ILC design for uncertain linear systems with time-varying delays and random packet dropouts. This design transformed the ILC design into a robust stability problem for a 2-D stochastic system through the LMI form of the delay-dependent stability condition. Yan *et al.* [33] proposed an ILC scheme using the Lyapunov approach for a class of nonlinearly parametric time-delay systems with initial state errors. This method compensated for the nonlinearly parametric time-delay uncertainties.

The control input delay generally exists in control engineering applications, and it has not been studied in depth in the ILC control scheme design for nonlinear systems. The control input delay is often related to the control implementation issues in many industrial processes; thus, it affects the tracking performance in the ILC design. From this perspective, there are still many problems that need to be studied. One problem is how to get an effective update law for nonlinear systems while requiring less prior knowledge of the plant. Li *et al.* [34] investigated the convergence and robustness of a P-type ILC design for nonlinear discrete-time systems with multiple input delays, which resolved the main problem. However, this method has obvious shortcomings: the tracked trajectory is also assumed to have an identical delay model, and the update law requires the delay information. This P-type ILC design method was improved in [35]. However, in the improved design, the update law still needs the minimum delay information. Meanwhile, corrective measures for the iterative initial error and external disturbances were added, and the error inequalities were reconstructed from a compact form of 2-D linear inequalities [35]. Hao *et al.* [36], [37] proposed a robust ILC method using a 2-D system description of batch process operation for industrial batch processes with input delay. To compensate for the input delay, a 2-D state predictor was established to predict the augmented system states. Delay-dependent stability conditions were established according to LMIs. However, the conditions must be satisfied that the delay-free part of the 2-D system can be stabilized in the absence of uncertainties. Importantly, their work is only effective for discrete linear uncertain systems.

Therefore, this work focused on the stability and convergence of a robust ILC control design for continuous nonlinear systems with unknown control input delay. First, a sliding mode surface, i.e., iterative integral sliding mode (IISM), was designed to cause the convergence of the tracking error. It can cause the tracking error to continuously converge with the iteration process and eliminate the reaching phase from the initial time instant. Correspondingly, an ILC controller composed of the known vector and the unknown vector was given, in which the unknown was updated by the update law in the iterations. Then, the convergence analysis was performed, and the convergence conditions in both the time domain and the iteration domain were obtained. Furthermore, the chattering-free problem was considered, and the corresponding measures were listed. The measures leading to nonideal sliding mode were investigated to observe the effect on the tracking error converging. Finally, the design was applied to a one-link robotic manipulator control system and a vertical three-tank system, and its performance was verified through the application simulation results.

The contributions of this research are as follows.

1) *IISM Was Proposed:* It has the advantage of no reaching phase, and therefore, the tracking error in the reaching phase of the sliding mode can be eliminated. In addition, the proposed IISM has the iterative action; thus, the tracking error under the sliding mode converges to zero as the iteration time approaches infinity.
2) A robust ILC control design based on the IISM was proposed for a class of nonlinear systems with unknown control input delay. It guarantees the convergence of the sliding mode and the tracking error in both the time domain and the iteration domain while rejecting the unrepeatable disturbance. The design conquers the control input time delay, and the convergence conditions

are independent of the time delay. Therefore, the design does not require any delay-related assumptions except the delay itself.

The rest of this article is organized as follows. First, the problem is described in Section II. Then, in Section III, the design of an IISM surface is described, and its ideal sliding mode dynamics are analyzed. Next, in Section IV, the ILC controller design based on the IISM is presented, and the method of the design to ensure the reachability of the IISM in the time domain is analyzed. Subsequently, in Section V, the CEF is used to prove the convergence of the sliding mode and tracking error in the iteration domain. The chattering-free problem of the presented ILC design is synthesized in Section VI. Finally, the application simulation results of a one-link robotic manipulator and a vertical three-tank system are used to verify the control design in Sections VII and VIII, respectively, and the conclusions are drawn in Section IX.

## II. Problem Formulation

Consider a special class of nonlinear systems with parametric uncertainty and control input delay

$$\left.\begin{aligned} &\dot{x}_{k,i} = x_{k,i+1}, \quad i = 1, 2, \ldots, n-1 \\ &\dot{x}_{k,n} = \theta^T(t)\xi(x_k, t) + b(t)u_k(t-\tau) + \phi(x_k, t) \\ &y_k(t) = x_{k,1}(t) \end{aligned}\right\} \tag{1}$$

for $t \in [0, \ T]$, where $x_k(t) = [x_{k,1}, x_{k,2}, \ldots, x_{k,n}]^T$ is the measured state vector, $u_k(t) \in \mathbb{R}$ is the single control input signal, $\xi(x_k, t) \in \mathbb{R}^p$ is the known nonlinear field vector, $\theta(t) \in C^p(\mathbb{R})$ is the unknown time-varying parameter vector, $b(t) \in C(\mathbb{R})$ is the unknown nonlinear control gain vector, $\phi(x_k, t) \in \mathbb{R}$ represents unknown unrepeatable modeling uncertainties and external disturbances, $y_k(t)$ denotes the output, $k$ represents the $k$th iteration, $\tau \in \mathbb{R}$ is the unknown time delay of the control input, and $p \in \mathbb{R}$ is a known positive scalar.

The control task is to make the output $y_k(t)$ track a predesigned trajectory $y_d(t)$ $\forall t \in [0, T]$, and its state vector is $x_d(t) = [y_d, \dot{y}_d, \ldots, y_d^{(n-1)}]^T = [x_{d,1}, x_{d,2}, \ldots, x_{d,n}]^T$. The tracking must be repeatable and completed within a time interval $[0, T]$.

The system parts are considered to satisfy the following assumptions.

*Assumption 1:* The system nonlinear function $f(x_k, t) := \theta^T(t)\xi(x_k, t)+\phi(x_k, t)$ satisfies the global Lipschitz continuity condition.

*Assumption 2:* $b(t) > 0$ is continuously differentiable $\forall t \in [0, T]$.

*Assumption 3:* $\|\phi(x_k, t)\| \le d_m(t)$ with the scalar function $d_m(t) > 0$ $\forall t \in [0, T]$. Sometimes, $d_m(t)$ is a constant scalar $d_m$ that denotes the upper boundary.

*Assumption 4:* The parameter vector $\theta(t)$ has the upper bound, i.e., $\|\theta(t) \| \le \theta_m$ with $\theta_m$ is the known constant scalar.

*Assumption 5:* The time delay satisfies $0 \le \tau \le \tau_m < T$, where $\tau_m$ is some unknown constant scalar.

*Assumption 6:* The predesigned trajectory $y_d(t)$ is $n$-order continuously differentiable $\forall t \in [0, T]$.

In this article, $\|\cdot\|$ represents the Euclidean norm.

The initial conditions of our ILC design are as follows.

*Assumption 7:* The system state is with identical initial conditions, $x_k(0) = x(0), k = 0, 1, \ldots$, and satisfies the initial resetting condition, i.e., $x_k(0) = x(0) = x_d(0)$.

*Assumption 8:* $u(t) = 0 \forall t \in [-\tau, 0)$.

*Assumption 9:* $\xi(0, t) = 0$ $\forall t \in [0, \ T]$.

*Assumption 10:* $\phi(0, t) = 0$ $\forall t \in [0, \ T]$.

In practice, the control gain $b(t)$ cannot be infinite or zero. Therefore, the following assumption is required for the unknown control gain $b(t)$.

*Assumption 11:* The control gain $b(t)$ has the minimum value except for the upper bound $b_m$, i.e., $0 < \epsilon \le b(t) \le b_m$. Moreover, its time derivative has a boundary

$$|\dot{b}(t)| \le \bar{b}_m.$$

## III. IISM Design

Based on the control problem description in Section II, the dynamic of the tracking error $e_k(t) = x_d(t) - x_k(t)$ is

$$\begin{cases} \dot{e}_{k,i} = e_{k,i+1}, \quad i = 1, 2, \ldots, n-1 \\ \dot{e}_{k,n} = y_d^{(n)} - \theta^T(t)\xi(x_k, t) - b(t)u_k(t-\tau) - \phi(x_k, t) \end{cases} \tag{2}$$

which can be written as

$$\begin{cases} \dot{e}_k(t) = Ae_k(t) + B[y_d^{(n)} - \theta^T(t)\xi(x_k, t) \\ \qquad\qquad - b(t)u_k(t-\tau) - \phi(x_k, t)] \end{cases} \tag{3}$$

where

$$A = \begin{bmatrix} 0 & 1 & \cdots & 0 \\ \vdots & \ddots & \ddots & \vdots \\ 0 & \cdots & 0 & 1 \\ 0 & \cdots & 0 & 0 \end{bmatrix}, \quad B = \begin{bmatrix} 0 \\ \vdots \\ 0 \\ 1 \end{bmatrix}.$$

It can be seen that $(A, B)$ is controllable.

In this section, the IISM design is proposed and compared with the integral sliding mode (ISM) without iteration actions.

### A. IISM Switching Surface Design

The IISM switching surface is proposed as

$$\begin{aligned} s_k(t) = C^T[e_k(t) \ - e_k(0)] \\ + \int_0^t \big[(K^T - C^TA)e_k(\iota) \\ + K_p^T e_{k-1}(\iota) - Qs_k(\iota) - G\text{sgn}s_k(\iota)\big]d\iota \end{aligned} \tag{4}$$

where $e_k(0) = x_d(0) - x_k(0)$ is the initial value of the tracking error vector; $C \in \mathbb{R}^n$ is a predesigned parameter vector that makes that $C^TB = 1$ and $K, K_p \in \mathbb{R}^n$ are the designed parameter vectors that will be addressed in Section III-B; $Q > 0$ and $G > 0$ are all scalar constants to be selected for determining the convergence of $s_k(t)$ that will be addressed in Sections IV and V; sgn$(\cdot)$ denotes the symbolic function; and $\iota$ represents the integration variable.

The definition of the IISM (4) is a causal dynamic system, whose flow diagram is shown in Fig. 1. Its inputs come from $e_k(t), e_k(0), e_{k-1}(t)$, and its output is $s_k(t)$.

It is obvious that $s_k(0) = 0$, which means that the initial value of the sliding mode is on the origin.

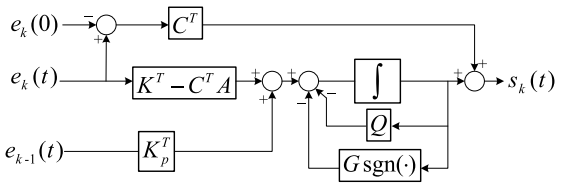


Fig. 1. IISM dynamic diagram.

According to (4), it can be got that

$$s_k(t) = \int_0^t \big[C^T \dot{e}_k(\imath) + (K^T - C^T A)e_k(\imath) + K_p^T e_{k-1}(\imath) - Qs_k(\imath) - G\mathrm{sgn}s_k(\imath)\big]d\imath$$

and

$$\dot{s}_k(t) = y_d^{(n)} - \theta^T(t)\xi(x_k,t) - b(t)u_k(t-\tau) - \phi(x_k,t) + K^T e_k(t) + K_p^T e_{k-1}(t) - Qs_k(t) - G\mathrm{sgn}s_k(t) \quad (5)$$

by using (3).

If the controller $u_k(t-\tau)$ drives the tracking error $e_k(t)$ on to the sliding mode surface and makes it remains there ideally, the sliding modes $s_k(t) = 0$ and $\dot{s}_k(t) = 0$. It means that

$$y_d^{(n)} - \theta^T(t)\xi(x_k,t) - b(t)u_k(t-\tau) - \phi(x_k,t) + K^T e_k(t) + K_p^T e_{k-1}(t) = 0.$$

Then, the equivalent control is achieved as

$$u_{k,eq}(t-\tau) = b^{-1}(t)\big[y_d^{(n)} - \theta^T(t)\xi(x_k,t) - \phi(x_k,t) + K^T e_k(t) + K_p^T e_{k-1}(t)\big]. \quad (6)$$

Substituting (6) into (3), we get the dynamic equation of $e_k(t)$ under the ideal sliding mode

$$\dot{e}_k(t) = (A - BK^T)e_k(t) - BK_p^T e_{k-1}(t) \quad (7)$$

which shows us that it can easily be a convergent process if the parameter vector $K$ is set to make $A - BK^T$ stable.

From (7), it can be seen that when the ideal sliding modes $s_k(t) = 0$ and $\dot{s}_k(t) = 0$ are reached, the tracking error dynamic under the sliding mode (4) is an iterative linear dynamic process. The tracking error of the previous iteration $e_{k-1}(t)$ will fix the tracking error $e_k(t)$ of the next iteration.

*Remark 1:* The proposed IISM is a dynamic subsystem with self-feedback and uses $e_k(t)$ and $e_{k-1}(t)$ as its inputs. Therefore, its dynamic contains iterative action of the tracking error and leads to a linear dynamic (7) in both the time and iteration domains, while the tracking error stays on the sliding mode surface $s_k(t) = 0$.

### B. Tracking Error Convergence Under the Sliding Mode

*Theorem 1:* Under Assumptions 1–10, the tracking error of the dynamic (2) in the ideal sliding modes $s_k(t) = 0$ and $\dot{s}_k(t) = 0$ converges to the origin as the iteration number approaches to infinity, that is

$$\lim_{k\to\infty} e_k(t) = 0$$

if there exist the appropriate sliding mode parameters $K$ and $K_p$ and the positive definite symmetric matrices $P$ and $R$ that make the inequality

$$\begin{bmatrix} \bar{A}^T P + P\bar{A} + R & -PBK_p^T \\ * & -R \end{bmatrix} < 0 \quad (8)$$

holds where $\bar{A} = A - BK^T$.

*Proof:* Select a Lyapunov function of $e_k(t)$ along with the dynamic (7) in the ideal IISM sliding mode as

$$V_k^m(t) = e_k^T(t)Pe_k(t) + \int_0^t e_k^T(\imath)Re_k(\imath)d\imath. \quad (9)$$

Seeking for its difference along the iterations

$$\begin{aligned}
\Delta V_k^m(t) &= e_k^T(t)Pe_k(t) - e_{k-1}^T(t)Pe_{k-1}(t) \\
&\quad + \int_0^t \big[e_k^T(\imath)Re_k(\imath) - e_{k-1}^T(\imath)Re_{k-1}(\imath)\big]d\imath \\
&= \int_0^t \big[\dot{e}_k^T(\imath)Pe_k(\imath) + e_k^T(\imath)P\dot{e}_k(\imath)\big]d\imath \\
&\quad + e_k^T(0)Pe_k(0) - e_{k-1}^T(t)Pe_{k-1}(t) \\
&\quad + \int_0^t \big[e_k^T(\imath)Re_k(\imath) - e_{k-1}^T(\imath)Re_{k-1}(\imath)\big]d\imath \\
&= \int_0^t e_k^T(\imath)[\bar{A}^T P + P\bar{A} + R]e_k(\imath)d\imath \\
&\quad - 2\int_0^t e_k^T(\imath)PBK_p^T e_{k-1}(\imath)d\imath \\
&\quad - \int_0^t e_{k-1}^T(\imath)Re_{k-1}(\imath)d\imath - e_{k-1}^T(t)Pe_{k-1}(t) \\
&= \int_0^t \begin{bmatrix} e_k(\imath) \\ e_{k-1}(\imath) \end{bmatrix}^T \begin{bmatrix} \bar{A}^T P + P\bar{A} + R & -PBK_p^T \\ * & -R \end{bmatrix} \begin{bmatrix} e_k(\imath) \\ e_{k-1}(\imath) \end{bmatrix} d\imath \\
&\quad - e_{k-1}^T(t)Pe_{k-1}(t).
\end{aligned}$$

The difference $\Delta V_k^m(t) < 0$ between the two iterations except that $e_k(t) = 0, e_{k-1}(t) = 0$, if the inequality (8) is satisfied. The tracking error $e_k(t)$ will converge to zero along with the iteration $k \to \infty$ according to the Lyapunov stability theory. ■

### C. ISM Switching Surface Design Without Iteration

To analyze the affection of iteration in the sliding mode, we describe the ISM without iteration in the following.

By deleting the iteration item about $e_{k-1}(t)$ in (4), i.e., $K_p = 0$

$$s_k(t) = C^T[e_k(t) - e_k(0)] + \int_0^t [(K^T - C^T A)e_k(\imath) - Qs_k(\imath) - G\mathrm{sgn}s_k(\imath)]d\imath \quad (10)$$

is got, and by (6), the equivalent control in the sliding mode $s_k(t) = 0$ and $\dot{s}_k(t) = 0$ is

$$u_{k,eq}(t-\tau) = b^{-1}(t)\big[y_d^{(n)} - \theta^T(t)\xi(x_k,t) - \phi(x_k,t) + K^T e_k(t)\big]. \quad (11)$$

Consequently, the dynamic equation of $e_k(t)$ in the ideal sliding mode becomes

$$\dot{e}_k(t) = (A - BK^T)e_k(t) \quad (12)$$

which shows that it is a stable time process without iteration.

However, the controller (6) or (11) is an analytic one that only exists on the theoretic layer. It cannot be implemented because of too much unknown information.

## IV. ILC Controller Design

The ILC controller is designed as

$$u_k(t) = \hat{\vartheta}_k^T(t)\psi(t) \tag{13}$$

where

$$\psi(t) = \left[\xi^T(x_k,t), y_d^{(n)} + K^T e_k(t) + K_p^T e_{k-1}(t), 0.5s_k(t)\right]^T \tag{14}$$

is a known smooth dynamic function vector and $\hat{\vartheta}_k(t)$ is the estimation of the unknown dynamic vector

$$\vartheta(t) = [-b^{-1}(t)\theta^T(t), b^{-1}(t), -b^{-2}(t)\dot{b}(t)]^T \tag{15}$$

which is a time-varying parameter vector to be updated by the learning algorithm (update law)

$$\hat{\vartheta}_k(t) = \hat{\vartheta}_{k-1}(t) + \psi(t)[\beta_1 s_k(t) + \beta_2 \mathrm{sgn}s_k(t)] \tag{16}$$

where $\beta_1$ and $\beta_2$ are all arbitrary-design positive scalars.

*Remark 2:* The controller (13) has the advantages of both the ILC controller and the SMC controller. It updates its learning parameter vector $\hat{\vartheta}_k(t)$ in every iteration according to the update law (16) and eventually completes the unknown information learning and makes the sliding mode value $s_k(t)$ converge to zero from the initial time constant. On the other hand, it has the essential SMC character in the time domain because part of the sliding mode $s_k(t)$ contains the high gain control function, which can reject the unrepeatable modeling uncertainty and disturbance $\phi(x_k,t)$.

Then, it follows the Razumikhin theories and theorems on the solution of retarded functional differential equation (RFDE) [38]. Because $\hat{\vartheta}_k(t)$ and $\psi(t)$ are function vectors of $e_k(t)$ and $x_k(t)$, there exist a constant $q > 1$ such that

$$\left\|\hat{\vartheta}_k^T(t-\tau)\psi(t-\tau)\right\| \le q\left\|\hat{\vartheta}_k^T(t)\psi(t)\right\| \tag{17}$$

for any solution of system (1) or (2). The similar application may refer to [39]. Based on this, the stability and convergence analysis are given as follows.

### A. Reachability of the IISM in Time Domain

*Theorem 2:* The IISM (4) reaches $s_k(t) = 0$ from the initial time instant under the ILC controller (13) if the parameter $G$ of the sliding mode surface satisfies that

$$G \ge d_m + b_m q\left\|\hat{\vartheta}_k^T(t)\psi(t)\right\| + b_m\|(\vartheta(t) - \hat{\vartheta}_k(t))^T\psi(t)\| \tag{18}$$

where $q > 2$ is the Razumikhin parameter that satisfies (17).

*Proof:* Consider a Lyapunov function at the $k$th iteration

$$V_k(t) = \frac{s_k^2(t)}{2b(t)} \tag{19}$$

and seek its derivative along the time domain

$$\begin{aligned}\dot{V}_k(t) &= b^{-1}(t)s_k(t)\dot{s}_k(t) - 0.5b^{-2}(t)\dot{b}(t)s_k^2(t)\\ &= s_k(t)[b^{-1}(t)\dot{s}_k(t) - 0.5b^{-2}(t)\dot{b}(t)s_k(t)].\end{aligned}$$

By (5), the above equation becomes

$$\begin{aligned}\dot{V}_k(t) = s_k(t)[&\vartheta^T(t)\psi(t) - u_k(t-\tau)\\ &- b^{-1}(t)\phi(x_k,t) - b^{-1}(t)Qs_k(t)\\ &- b^{-1}(t)G\mathrm{sgn}s_k(t)].\end{aligned}$$

Applying the controller (13) to the above, we have

$$\begin{aligned}\dot{V}_k(t) = s_k(t)\big[&(\vartheta^T(t) - \hat{\vartheta}_k^T(t))\psi(t) + \hat{\vartheta}_k^T(t)\psi(t)\\ &- \hat{\vartheta}_k^T(t-\tau)\psi(t-\tau)\\ &- b^{-1}(t)\phi(x_k,t) - b^{-1}(t)Qs_k(t)\\ &- b^{-1}(t)G\mathrm{sgn}s_k(t)\big].\end{aligned} \tag{20}$$

Based on (17), the following inequality is got:

$$\begin{aligned}\dot{V}_k(t) \le |s_k(t)|\big(&\|(\vartheta(t) - \hat{\vartheta}_k(t))^T\psi(t)\| + q\left\|\hat{\vartheta}_k^T(t)\psi(t)\right\|\big)\\ &+ b^{-1}(t)\big(d_m|s_k(t)| - Qs_k^2(t) - G|s_k(t)|\big).\end{aligned} \tag{21}$$

It is obvious that

$$\dot{V}_k(t) \le -b^{-1}(t)Qs_k^2(t) \tag{22}$$

stands if the condition (18) is satisfied, which means that the IISM (4) can be reached asymptotically. From (4), we know $s_k(0) = 0$, so the sliding mode is reached from the initial time instant and retains there. ■

*Remark 3:* From condition (18), it can be seen that the convergent character of the IISM (4) in the time domain is determined by the iteration approximation error $\hat{\vartheta}_k(t) - \vartheta(t)$.

*Corollary 1:* The IISM (4) reaches on $s_k(t) = 0$ from the initial time instant under the ILC controller (13) if the parameter $G$ of the sliding mode surface satisfies that

$$G \ge d_m + b_m\|(\vartheta(t) - \hat{\vartheta}_k(t))^T\psi(t)\| \tag{23}$$

and the control input time delay $\tau = 0$.

*Proof:* Based on the proof of Theorem 2, considering the Lyapunov function at the $k$th iteration the same as (19) and seeking its derivative along the time domain using (5) and (13), one gets

$$\begin{aligned}\dot{V}_k(t) \le |s_k(t)|(&\|(\vartheta(t) - \hat{\vartheta}_k(t))^T\psi(t)\| + b^{-1}(t)d_m|s_k(t)|\\ &- b^{-1}(t)Qs_k^2(t) - b^{-1}(t)G|s_k(t)|.\end{aligned}$$

It is obvious that

$$\dot{V}_k(t) \le -b^{-1}(t)Qs_k^2(t)$$

stands if condition (23) is satisfied, which means that the IISM (4) can be reached asymptotically. We know that $s_k(0) = 0$, so the sliding mode is reached from the initial time instant and retains there. ■

### B. Further Analysis

*Lemma 1:* The sliding mode (4) reaches on $s_k(t) = 0$ from the initial time instant under the ILC controller (13) if the parameter $G$ of the sliding mode surface satisfies that

$$G \ge d_m + b_m q\left\|\hat{\vartheta}_k^T(t)\psi(t)\right\| + \frac{b_m\|\psi(t)\|}{\epsilon^2}\sqrt{(1+\theta_m^2)\epsilon^2 + \bar{b}_m^2}. \tag{24}$$

*Proof:* According to (15) and Assumptions 4 and 11, the norm of $\vartheta(t)$ satisfies

$$\|\vartheta(t)\| \le \frac{1}{\epsilon^2}\sqrt{\epsilon^2(1+\theta_m^2) + \bar{b}_m^2}. \tag{25}$$

According to the proof of Theorem 2, condition (18) can be set as

$$G \geq d_m + b_m\big[(1+q)\big\|\hat{\vartheta}_k^T(t)\psi(t)\big\| + \|\vartheta^T(t)\psi(t)\|\big].$$

The scalar $q > 1$ is easily selected as $q = q + 1$ due to its unknownness by (17). Next, by using (25) into the above inequality, the overall proof of Theorem 2 still holds under condition (24). Lemma 1 is proved. ∎

*Remark 4:* It can be seen that the convergent character of the IISM (4) in the time domain is determined by the known information $\|\psi(t)\|$ and $\|\hat{\vartheta}_k(t)\|$. In addition, if the parameter $G$ meets the following condition:

$$G = d_m + b_m q\big\|\hat{\vartheta}_k^T(t)\psi(t)\big\| + \frac{b_m\|\psi(t)\|}{\epsilon^2}\sqrt{(1+\theta_m^2)\epsilon^2 + \bar{b}_m^2}$$

the convergence is independent on the approximation error in the iteration domain.

*Lemma 2:* The IISM (4) reaches on $s_k(t) = 0$ from the initial time instant under the ILC controller (13) if the parameter $G$ of the sliding mode surface satisfies that

$$G \geq d_m + \frac{b_m\|\psi(t)\|}{\epsilon^2}\sqrt{(1+\theta_m^2)\epsilon^2 + \bar{b}_m^2} \tag{26}$$

and the control input time delay $\tau = 0$.

*Proof:* According to the proof of Corollary 1, condition (18) can be set as

$$G \geq d_m + b_m\|\vartheta^T(t)\psi(t)\|.$$

Next, by using (25) for the above inequality, under condition (26), it is generally proved that Corollary 1 still holds. Thus, Lemma 2 is proved. ∎

*Remark 5:* The results of Theorem 2, Corollary 1, and Lemmas 1 and 2 can also work on the ISM without iteration (10). Whether the sliding mode (6) has the iteration action does not interfere with its reachability.

## V. Convergence Analysis

This section donates to the convergence in the iteration learning domain.

*Theorem 3:* For the tracking error system (2) under Assumptions 1–10, the ILC controller (13) with the update law (16) drives the IISM (4) of the closed-loop system asymptotically converging to the origin as the iteration number approaches to infinity, that is

$$\lim_{k\to\infty} s_k(t) = 0$$

if the sliding mode parameter $G$ satisfies

$$G \geq d_m + q b_m\|\hat{\vartheta}_k^T(t)\psi(t)\|. \tag{27}$$

*Proof:* Select the composite energy function (CEF) at the $k$th iteration as

$$J_k(t) = J_k^1(t) + J_k^2(t) + J_k^3(t) \tag{28}$$

where

$$J_k^1(t) = \frac{\beta_1}{2b(t)}s_k^2(t), \quad J_k^2(t) = \frac{\beta_2}{b(t)}|s_k(t)|$$
$$J_k^3(t) = \frac{1}{2}\int_0^t \tilde{\vartheta}_k^T(\iota)\tilde{\vartheta}_k(\iota)d\iota \tag{29}$$

with $\tilde{\vartheta}_k(t) = \vartheta(t) - \hat{\vartheta}_k(t)$.

Seek the difference of $J_k(t)$ between two successive iterations $k$ and $k-1$

$$\begin{aligned}\Delta J_k(t) &= J_k(t) - J_{k-1}(t)\\ &= \Delta J_k^1(t) + \Delta J_k^2(t) + \Delta J_k^3(t)\end{aligned} \tag{30}$$

where the difference items $\Delta J_k^1(t)$, $\Delta J_k^2(t)$, and $\Delta J_k^3(t)$ are deduced as follows.

By (29) and using (16), (19), and (20), the following difference is got:

$$\begin{aligned}\Delta J_k^1(t) &= \beta_1\int_0^t \dot{V}_k(\iota)d\iota - \beta_1 V_{k-1}(t)\\ &= \beta_1\int_0^t s_k(\iota)\big[\tilde{\vartheta}_k^T(\iota)\psi(\iota) + \Delta u_k^\tau(\iota)\big]d\iota\\ &\quad - \beta_1\int_0^t b^{-1}(\iota)\phi(x_k,\iota)s_k(\iota)d\iota\\ &\quad - \beta_1\int_0^t b^{-1}(\iota)G|s_k(\iota)|d\iota\\ &\quad - \beta_1\int_0^t b^{-1}(\iota)Qs_k^2(\iota)d\iota - \beta_1 V_{k-1}(t)\end{aligned} \tag{31}$$

where $\Delta u_k^\tau(t) = \hat{\vartheta}_k^T(t)\psi(t) - \hat{\vartheta}_k^T(t-\tau)\psi(t-\tau)$.

By (29) and according to (5) and (13)–(15), the following difference is got:

$$\begin{aligned}\Delta J_k^2(t) &= \beta_2\int_0^t [b^{-1}(\iota)|s_k(\iota)|]_\iota' d\iota - J_{k-1}^2(t)\\ &= \beta_2\int_0^t \mathrm{sgn}s_k(\iota)\big[\tilde{\vartheta}_k^T(\iota)\psi(\iota) + \Delta u_k^\tau(\iota)\big]d\iota\\ &\quad - \beta_2\int_0^t b^{-1}(\iota)\phi(x_k,\iota)\mathrm{sgn}s_k(\iota)d\iota\\ &\quad - \beta_2\int_0^t b^{-1}(\iota)G\mathrm{sgn}^2 s_k(\iota)d\iota\\ &\quad - \beta_2\int_0^t b^{-1}(\iota)Q|s_k(\iota)|d\iota - J_{k-1}^2(t).\end{aligned} \tag{32}$$

By (29) and according to the definition of $\tilde{\vartheta}_k(t)$, the following difference is got:

$$\begin{aligned}\Delta J_k^3(t) &= \frac{1}{2}\int_0^t \big[\tilde{\vartheta}_k^T(\iota)\tilde{\vartheta}_k(\iota) - \tilde{\vartheta}_{k-1}^T(\iota)\tilde{\vartheta}_{k-1}(\iota)\big]d\iota\\ &= \frac{1}{2}\int_0^t [\tilde{\vartheta}_k(\iota) - \tilde{\vartheta}_{k-1}(\iota)]^T\\ &\quad \times [\tilde{\vartheta}_k(\iota) - \tilde{\vartheta}_{k-1}(\iota) + 2\tilde{\vartheta}_{k-1}(\iota)]d\iota\\ &= \frac{1}{2}\int_0^t [\hat{\vartheta}_{k-1}(\iota) - \hat{\vartheta}_k(\iota)]^T\\ &\quad \times [2(\vartheta(\iota) - \hat{\vartheta}_k(\iota)) + \hat{\vartheta}_k(\iota) - \hat{\vartheta}_{k-1}(\iota)]d\iota\\ &= \int_0^t [\vartheta(\iota) - \hat{\vartheta}_k(\iota)]^T[\hat{\vartheta}_{k-1}(\iota) - \hat{\vartheta}_k(\iota)]d\iota\\ &\quad - \frac{1}{2}\int_0^t \|\hat{\vartheta}_k(\iota) - \hat{\vartheta}_{k-1}(\iota)\|_2^2 d\iota.\end{aligned} \tag{33}$$

Then, substituting the update law (16) into (33), we get the following difference:

$$\begin{aligned}\Delta J_k^3(t) &= -\beta_1\int_0^t s_k(\iota)\tilde{\vartheta}_k^T(\iota)\psi(\iota)d\iota\\ &\quad - \beta_2\int_0^t \tilde{\vartheta}_k^T(\iota)\psi(\iota)\mathrm{sgn}s_k(\iota)d\iota\\ &\quad - \frac{1}{2}\int_0^t \|\hat{\vartheta}_k(\iota) - \hat{\vartheta}_{k-1}(\iota)\|_2^2 d\iota.\end{aligned} \tag{34}$$

Substituting the difference results (31), (32), and (34) of $J_k^1(t)$, $J_k^2(t)$, and $J_k^3(t)$, respectively, into (30), we get the difference of the CEF (28) as follows:

$$\begin{aligned}\Delta J_k(t) = {} & \beta_1 \int_0^t \left[\Delta u_k^\tau(\iota) - b^{-1}(\iota)\phi(x_k,\iota)\right] s_k(\iota)d\iota \\ & + \beta_2 \int_0^t \left[\Delta u_k^\tau(\iota) - b^{-1}(\iota)\phi(x_k,\iota)\right] \mathrm{sgn} s_k(\iota)d\iota \\ & - \beta_1 \int_0^t b^{-1}(\iota) Q s_k^2(\iota)d\iota \\ & - \int_0^t b^{-1}(\iota)(\beta_1 G + \beta_2 Q)|s_k(\iota)|d\iota \\ & - \beta_2 \int_0^t b^{-1}(\iota) G \mathrm{sgn}^2 s_k(\iota)d\iota - \beta_1 V_{k-1}(t) \\ & - J_{k-1}^2(t) - \frac{1}{2}\int_0^t \|\hat{\vartheta}_k(\iota) - \hat{\vartheta}_{k-1}(\iota)\|_2^2 d\iota. \end{aligned} \tag{35}$$

The norm of the difference $\Delta u_k^\tau(t)$ between the time $t$ and $t-\tau$ can be got as

$$\left\|\Delta u_k^\tau(t)\right\| \le q\left\|\hat{\vartheta}_k^T(t)\psi(t)\right\|$$

by the principle of (17), where $q > 2$ is the existing unknown Razumikhin scalar constant. Thus, applying condition (27) into (35), one can easily conclude that

$$\Delta J_k(t) < 0$$

except $J_k(t) = 0$. Therefore, the sliding mode $s_k(t)$ will be driven to the origin along the successive iterations if $k \to \infty$. The proof is completed. ■

It is obvious that the following result holds based on Theorem 3.

*Corollary 2:* For the tracking error system (2) under Assumptions 1–10, the ILC controller (13) with the update law (16) drives the IISM (4) of the closed-loop system asymptotically converging to the origin as the iteration number approaches to infinity, that is

$$\lim_{k\to\infty} s_k(t) = 0$$

if the control time delay $\tau = 0$ and the sliding mode parameter $G$ satisfy

$$G \ge d_m. \tag{36}$$

*Proof:* Based on the proof of Theorem 3, consider the same CEF at the $k$th iteration as (28) and seek the difference of $J_k(t)$ between two successive iterations. Because the control input time delay is $\tau = 0$, $\Delta u_k^\tau(t) = 0$. Consequently, we get the difference of the CEF (28) as follows:

$$\begin{aligned}\Delta J_k(t) = {} & -\int_0^t [\beta_1\ s_k(\iota) + \beta_2 \mathrm{sgn} s_k(\iota)] b^{-1}(\iota)\phi(x_k,\iota)d\iota \\ & - \beta_1 \int_0^t b^{-1}(\iota) Q s_k^2(\iota)d\iota \\ & - \int_0^t b^{-1}(\iota)(\beta_1 G + \beta_2 Q)|s_k(\iota)|d\iota \\ & - \beta_2 \int_0^t b^{-1}(\iota) G \mathrm{sgn}^2 s_k(\iota)d\iota - \beta_1 V_{k-1}(t) \\ & - J_{k-1}^2(t) - \frac{1}{2}\int_0^t \|\hat{\vartheta}_k(\iota) - \hat{\vartheta}_{k-1}(\iota)\|_2^2 d\iota. \end{aligned}$$

If the condition $G \ge d_m$ is applied to the above, $\Delta J_k(t) < 0$ is got. Therefore, Corollary 2 is proved. ■

*Remark 6:* Compared with that of the time domain (16), the iteration convergence condition (27) eliminates the information of the approximation $\tilde{\vartheta}_k(t)$. However, it includes the necessary rejecting forces to the unrepeatable disturbance or unmodeled dynamics and to the redundancy resulted from the time delay $\tau$. If $\tau = 0$ and the unrepeatable disturbance is $\phi(x_k,t) = 0$, the parameter $G \ge 0$ is enough to guarantee the convergence in the iteration learning. This characteristic determines that the sliding mode design parameter $G$ is important both in the time domain and the iteration domain. In addition, it can be considered that the treatment for the time delay is transferred to $G$.

*Remark 7:* In practice, the parameter $G$ can be selected or designed as follows. Because the value of the scalar $q > 2$ is unknown and only exists theoretically, it can be estimated. Therefore, we can select

$$G = d_m + (2+\varepsilon) b_m \left\|\hat{\vartheta}_k^T(t)\psi(t)\right\| \tag{37}$$

where $\varepsilon > 0$ is the arbitrary tuning scalar according to the situation of the time delay.

*Remark 8:* Note that the results in this article are not changed while using $d_m(t)$ to replace of $d_m$ according to Assumption 3.

## VI. Measures for Chattering Free

As we were known, SMC control always contains chattering problems due to its high gain control character for rejecting disturbance. Therefore, there is a chattering problem in our method. The switching actions are inherent in the signal of sgn(·).

The proposed sliding mode ILC control contains two types of chattering phenomena. One is in the iteration domain, which is caused by the update law (16) that includes the signal of sgn(·). Another is in the time domain, which is due to the action of the controller (13). The chattering in the time domain is not easy to analyze because the signal of sgn(·) rests on the IISM (4). However, when the IISM is kept at the origin by the controller (13), the situation becomes not satisfactory. Any slight action can cause the deviation of the ideal sliding mode. Then, the signal of sgn(·) will produce a switching action with an amplitude of $G$. Although it is filtered by the integral function, which reduces switching frequency, its switching amplitude becomes larger. Especially, the value of the chattering $s_k(t)$ is used to the update law (16). Therefore, the control action includes a chattering phenomenon in the time domain. If one wants to guarantee the reachability of the IISM (4) in the time domain, according to conditions (18) and (23) or (24) and (26), the parameter $G$ needs to be bigger to get the high-gain control action.

Three measures for chattering free were taken.

1) *Minimizing the Parameter G:* As controller (13) can learn to stabilize the sliding mode $s_k(t)$, the IISM (4) does not need to quickly converge in the time domain. Therefore, if $\tau = 0$, we set $G$ to satisfy condition (27) or (36).

2) *Minimizing the Parameter $\beta_2$:* Although the parameter $\beta_2$ has the iterative learning function, it causes the chattering phenomenon in both the iteration domain and the time domain. Its original function is to accelerate the convergence and guarantee the reachability of the IISM (4), which is useful under the condition of unpredictable disturbance in the iteration domain. However, the value of $\beta_2$ is not easy to be selected because of the unpredictable counterparts. Simulation result has shown that it can make the learning process fluctuate within a certain area between adjacent iterations, that is, the chattering occurs in the iteration domain.
3) *Using the Saturation Function sat$(\cdot)$ to Replace the sgn$(\cdot)$:* It is a classical method to solve the chattering problem of the SMC control method. The saturation function is expressed as

$$\text{sat}s_k(t) = \begin{cases} 1, & s_k(t) \geq \varphi \\ s_k(t)/\varphi, & |s_k(t)| < \varphi \\ -1, & s_k(t) \leq -\varphi. \end{cases} \tag{38}$$

When $|s_k(t)| \geq \varphi$, sat$(\cdot)$ can be considered as the same function as sgn$(\cdot)$. When $|s_k(t)| < \varphi$, sat$(\cdot)$ can be considered as a linear function of $s_k(t)$. In addition, the positive scalar $\varphi > 0$ is called the boundary layer of the sliding mode.

The above three measures were taken to overcome the chattering problem. Then, the IISM can be rewritten as follows using (5):

$$\begin{aligned} s_k(t) &= C^T[e_k(t) - e_k(0)] \\ &\quad + \int_0^t \big[(K^T - C^T A)e_k(\imath) \\ &\qquad + K_p^T e_{k-1}(\imath) - Qs_k(\imath) - G\text{sat}s_k(\imath)\big]d\imath \end{aligned} \tag{39}$$

and

$$\begin{aligned} \dot{s}_k(t) &= y_d^{(n)} - \theta^T(t)\xi(x_k, t) - b(t)u_k(t-\tau) - \phi(x_k, t) \\ &\quad + K^T e_k(t) + K_p^T e_{k-1}(t) - Qs_k(t) - G\text{sat}s_k(t). \end{aligned} \tag{40}$$

Due to the chattering free measure of saturation function, $s_k(t) \neq 0$, and $\dot{s}_k(t) \neq 0$. Undoubtedly, according to SMC theory, the IISM (39) will be located in the inner boundary layer under the ILC control (13), i.e., $|s_k(t)| \leq \varphi$. The corresponding tracking error is then analyzed as follows.

*Theorem 4:* For the tracking error system (2) with Assumptions 1–10, the tracking error within the sliding mode boundary layer $|s_k(t)| \leq \varphi$ satisfies

$$\lim_{k\to\infty} e_k(t) \leq \varphi \|[Is - \bar{A}]^{-1} B(s + Q + G/\varphi)\|_\infty \tag{41}$$

over $[0, T]$ as the iteration number approaches to infinity.

*Proof:* According to (38) and (40), the equivalent control of the controller is achieved as

$$\begin{aligned} &u_{k,eq}(t-\tau) \\ &= b^{-1}(t)\big[y_d^{(n)} - \theta^T(t)\xi(x_k, t) - \phi(x_k, t) + K^T e_k(t) \\ &\qquad + K_p^T e_{k-1}(t) - \dot{s}_k(t) - (Q + G/\varphi)s_k(t)\big] \end{aligned} \tag{42}$$

while the IISM is in the inner of the boundary layer $|s_k(t)| \leq \varphi$.

By substituting (42) into (3), we can get the dynamic equation of $e_k(t)$ within the sliding mode boundary layer

$$\begin{aligned} \dot{e}_k(t) &= (A - BK^T)e_k(t) - BK_p^T e_{k-1}(t) \\ &\quad + B[\dot{s}_k(t) + (Q + G/\varphi)s_k(t)] \end{aligned} \tag{43}$$

which shows us how the sliding mode value affects the tracking error. Its description the frequency domain is

$$(Is - \bar{A})E_k(s) = B(s + Q + G/\varphi)S_k(s) - BK_p^T E_{k-1}(s) \tag{44}$$

and obviously

$$\begin{aligned} E_k(s) &= (Is - \bar{A})^{-1} B(s + Q + G/\varphi)S_k(s) \\ &\quad - (Is - \bar{A})^{-1} BK_p^T E_{k-1}(s). \end{aligned}$$

According to Theorem 1, the sliding mode parameters satisfy condition (8), and then, $E_{k-1}(s)$ does not affect the tracking error value when $k \to \infty$. Therefore, the tracking error value in the frequency domain becomes

$$E_k(s) = (Is - \bar{A})^{-1} B(s + Q + G/\varphi)S_k(s)$$

when the iteration times $k \to \infty$. Then, (41) holds. The proof is completed. ■

*Remark 9:* Theorem 4 shows the effect of the nonideal sliding mode on the tracking error. Through (41), the parameter $G$ is most relevant to the tracking error when the iteration approaches infinity. This is the cost of rejecting the unrepeatable disturbance $\phi(x_k, t)$. According to (41), we can design a better parameter $K$ to make the minor bound of the tracking error.

## VII. Applicaiton Example I

Consider the following one-link robotic manipulator:

$$\begin{aligned} \dot{x}_{k,1} &= x_{k,2} \\ \dot{x}_{k,2} &= -\frac{gl}{ml^2 + J}\cos x_{k,1} + \frac{1}{ml^2 + J}u(t-\tau) + \phi(x_k, t) \\ x_k(0) &= x_0(0) \quad \forall t \in [0, 1] \end{aligned} \tag{45}$$

where $x_{k,1}$ is the joint angle, $x_{k,2}$ is the angular velocity, $x_k = [x_{k,1}, x_{k,2}]^T$ is the state vector, $m = (3 + 0.1\sin t)$ kg is the mass, $l = 1$ m is the length, $J = 0.5$ kg$\cdot$m$^2$ is the moment of inertia, and $\tau$ denotes the control input delay. According to (1), set $\xi(x_k, t) = \cos x_{k,1}$. $A = \left[\begin{smallmatrix} 0 & 1 \\ 0 & 0 \end{smallmatrix}\right]$ and $B = \left[\begin{smallmatrix} 0 \\ 1 \end{smallmatrix}\right]$ according to the math description (3). This robotic manipulator was from the literature [40].

The desired trajectory was selected as $x_{d,1} = y_d = \sin t$ and $x_d(0) = [0, 1]^T$. First, we designed the IISM surface by (39). In the predesign step, $C^T = [1, 1]$ was set to satisfy $C^T B = 1$, and $K^T = [800, 201]$ was set to ensure that $A - BK^T$ is a stable matrix. In addition, the tracking error conditions (8) and (41) were considered. The parameter $Q = 40$ was selected, and $s_k(t)$ at the $k$th iteration was got

$$\begin{aligned} s_k(t) &= e_{k,1}(t) + e_{k,2}(t) - e_{k,1}(0) - e_{k,2}(0) \\ &\quad + \int_0^t [800\ e_{k,1}(\imath) + 200\ e_{k,2}(\imath) + K_p^T e_{k-1}(\imath) \\ &\qquad - 40s_k(\imath) - G\text{sat}s_k(\imath)]d\imath. \end{aligned}$$

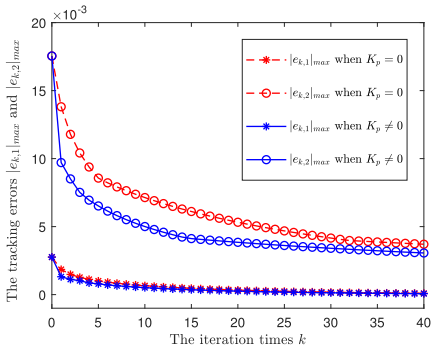


Fig. 2. Tracking error maximum values following the iteration times.

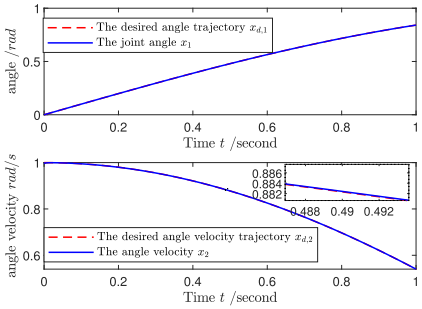


Fig. 3. Joint angle and angle velocity tracking curves.

The parameters $K_p$ and $G$ and the boundary layer $\varphi$ were set by different cases in the following.

### A. Simulation Results When $\tau = 0$

To validate our method and illustrate its merits, we first conducted the simulation when the time delay was $\tau = 0$ and then compared with the second-order sliding mode (second-order SM) ILC method in [40].

Let $x_k(0) = x_d(0)$ and $\phi(x_k, t) = 5\sin^3 t$. The disturbance was repeatable; thus, the parameter $G$ was set to $G = 0$ with $\varphi = 0$. The parameters of iterative learning in (16) were set to $\beta_1 = 20$ and $\beta_2 = 0$. First, $K_p = 0$ was set, i.e., the sliding mode did not have iterative action. Then, $K_p = [90, 120]^T$ was set. The trends of the maximum tracking error values with iteration times were obtained, as shown in Fig. 2. When $K_p \neq 0$, the tracking errors are smaller and converge faster than the results at $K_p = 0$, which demonstrates the function of the iterative action in the IISM. When $K_p = [90, 120]^T$, the tracking curves of the joint angle and angular velocity after iteration $k = 40$ are shown in Fig. 3. From the results, it is obvious that the rejecting control action is not required in the condition of the repeatable disturbance. The corresponding IISM converges over the iteration times are shown in Fig. 4. Then, we set $\beta_2 = 2$ to testify the chattering phenomenon caused by $\beta_2$. Fig. 5 shows that the sliding mode value is chattering within a neighbor of zero when $\beta_2 = 2$. However, the sliding mode converges faster in contrast with Fig. 4, and the tracking errors converge faster and have fluctuations due to $\beta_2 \neq 0$, as shown in Fig. 6. The corresponding control torque has a chattering phenomenon, as shown in Fig. 7.

Then, the tracking effects of the two methods were compared. The second-order sliding mode ILC in [40] was applied, and the parameters were set the same as in the literature. Fig. 8

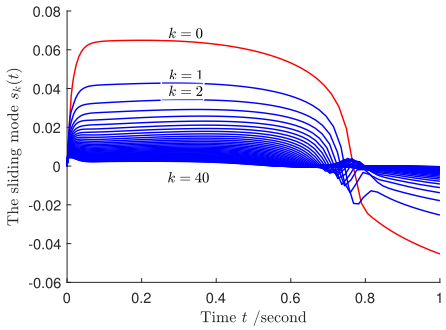


Fig. 4. IISM converging curves along with the iteration times.

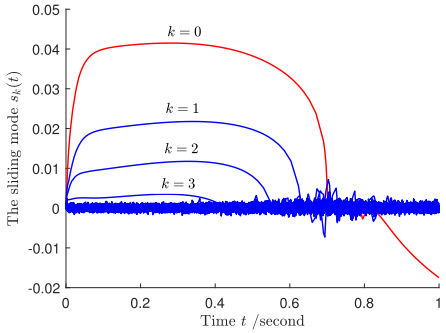


Fig. 5. IISM values when $\beta_2 = 2$.

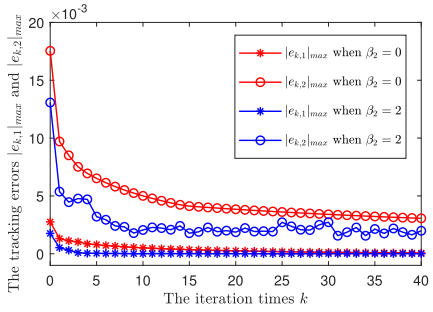


Fig. 6. Tracking error comparison when $\beta_2 = 0$ and $\beta_2 = 2$.

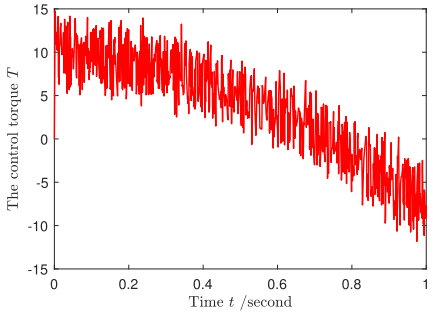


Fig. 7. ILC control torque based on IISM when $\beta_2 = 2$.

shows that the tracking errors of our IISM method are very smaller from the initial iteration time, while the tracking errors of the second-order sliding mode method are bigger from the initial iteration time. The comparisons of the sliding mode values and control torque values after $k = 40$ iteration between the IISM method and the second-order SM method are shown in Fig. 9 and Fig. 10, respectively. The results are also shown in Fig. 11. After 40 iterations, the error track in the phase plane of our method is obvious within a smaller range than the other method. This is because the IISM eliminates the reaching

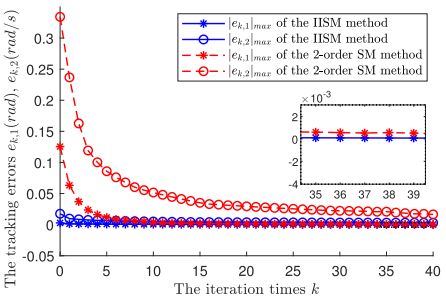


Fig. 8. Tracking error maximum values comparison following the iteration times between the IISM method and the second-order SM method.

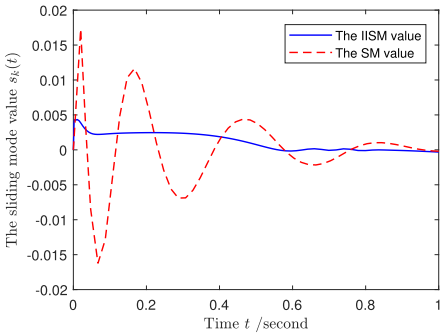


Fig. 9. Sliding mode values comparison after $k = 40$ iteration between the IISM method and the second-order SM method.

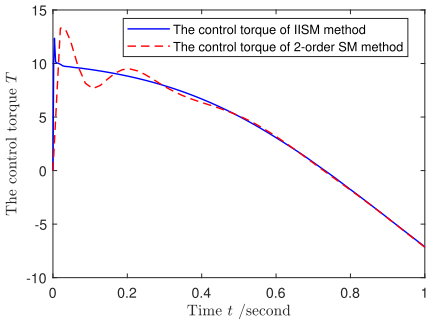


Fig. 10. Control torque values comparison after $k = 40$ iteration between the IISM method and the second-order SM method.

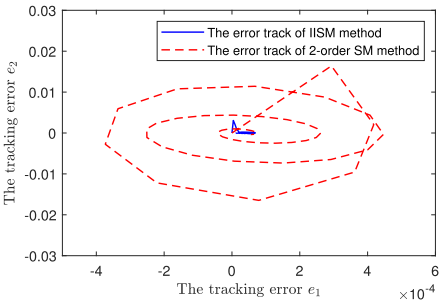


Fig. 11. Error track comparison in phase plane after $k = 40$ iteration between the IISM method and the second-order SM method.

phase of the sliding mode. Therefore, the ILC control method based on the IISM achieves the smaller tracking errors from the initial iteration times. This is its special advantage.

Consequently, we verified the ability of the IISM method to reject unrepeatable disturbance. First, we set $\phi(x_k, t) = 5d \sin^3 \omega t$, where the amplitude $d$ and frequency $\omega$ were randomly generated at the interval $(0, 1)$ in each iteration. Correspondingly, the parameters $G = 5.5$ and $\varphi = 0.01$ were

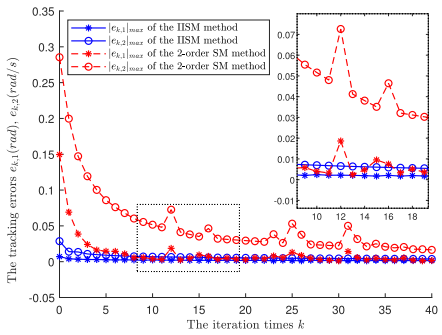


Fig. 12. Tracking error maximum values comparison following the iteration times between the IISM method and the second-order SM method.

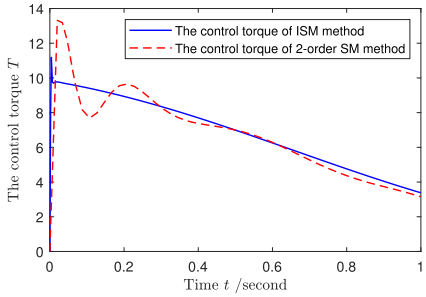


Fig. 13. Control torque values comparison after $k = 40$ iteration between the IISM method and the second-order SM method.

selected in the IISM. Then, the same second-order sliding mode ILC in [40] was applied under the same unrepeatable disturbance. The results are shown in Fig. 12. The IISM method can suppress the unrepeatable disturbance with minor ripple along the iteration times, while the second-order sliding mode method has bigger fluctuations along with the iterations. The corresponding control torques are shown in Fig. 13, which indicates that there is no chattering phenomenon in the control torque signal of the IISM method.

### *B. Simulation Results When $\tau \neq 0$*

When there is the control input time delay, the second-order sliding mode ILC method in [40] cannot be applied. We illustrate the results of the proposed IISM-based ILC method.

First, the control input time delay was set $\tau = 0.01$ s. There was no unrepeatable disturbance, i.e., $\varphi(x_k, t) = 0$. The following parameters were set: $\beta_1 = 0.1$, $\beta_2 = 0$, $G = 2.1\|\hat{\vartheta}_k^T(t)\psi(t)\|$, and $\varphi = 0.002$. The other parameters in the IISM and control law were set the same, as mentioned in this section. The simulation results are shown in Figs. 14–16. Although the joint angular velocity $x_2$ cannot track the reference signal $x_{d,2}$ perfectly from the initial time instant, the angle signal $x_1$ can track the reference signal $x_{d,1}$ perfectly, which is shown in Fig. 15. In addition, Fig. 16 shows that the sliding mode converges to the area within the boundary $\varphi = 0.002$ along with the iteration times $k$. To verify the effect of rejecting the unrepeatable disturbance, we set $\phi(x_k, t) = 5d \sin^3 \omega t$ to be the same in Section VII-A and obtain the result in Fig. 17, which shows the trends of the maximum tracking errors $|e_{k,1}|_{\max}$ and $|e_{k,2}|_{\max}$ along the iteration times $k$. It can be seen that the random unrepeatable disturbance only has minor effect on the tracking error.

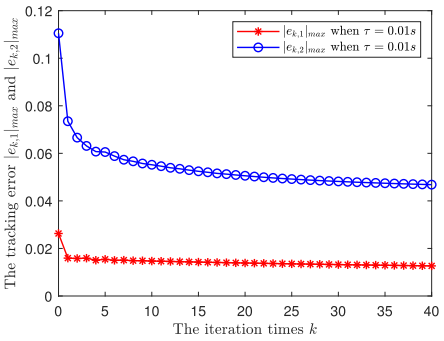


Fig. 14. Tracking error maximum values following the iteration times when the control input time delay $\tau = 0.01$ s.

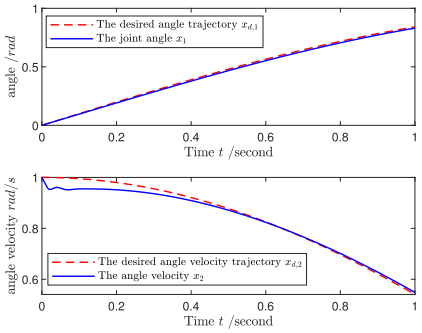


Fig. 15. Joint angle and angle velocity tracking curves when the control input time delay $\tau = 0.01$ s.

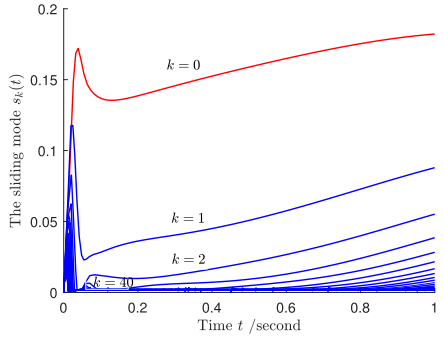


Fig. 16. IISM converging curves along with the iteration times when the control input time delay $\tau = 0.01$ s.

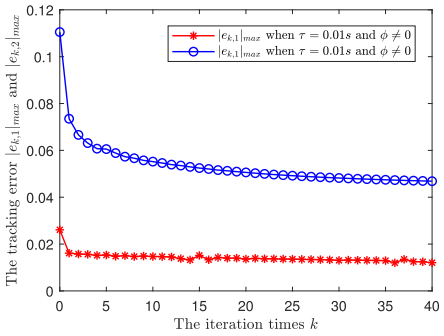


Fig. 17. Tracking error maximum values following the iteration times when the control input time delays $\tau = 0.01$ s and $\phi(x_k, t) = 5d \sin^3 \omega t$.

Then, the control input time delay was set to a bigger value $\tau = 0.1$ s. This is a big delay for the manipulator driving system. The ILC based on the IISM was applied to the one-link robotic manipulator. A bigger control input time delay caused greater tracking error. The learning parameter $\beta_1 = 0.004$ was

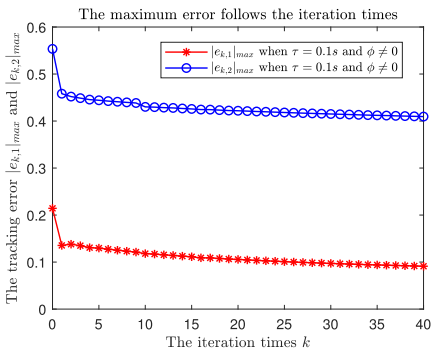


Fig. 18. Tracking error maximum values following the iteration times when the control input time delay $\tau = 0.1$ s and $\phi(x_k, t) = 5d \sin^3 \omega t$.

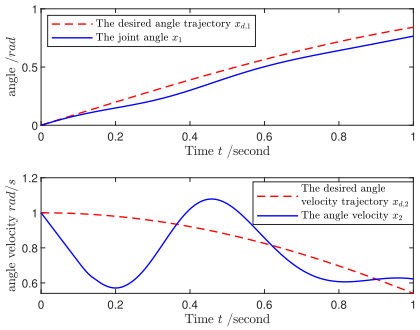


Fig. 19. Joint angle and angle velocity tracking curves when the control input time delay $\tau = 0.1$ s and $\phi(x_k, t) = 5d \sin^3 \omega t$.

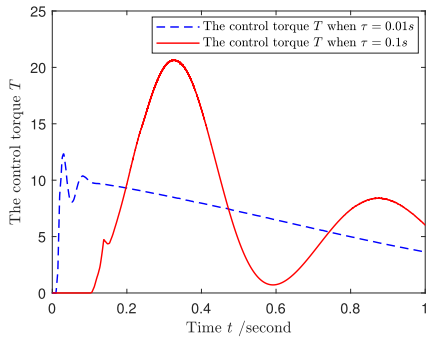


Fig. 20. Control torque curves when the control input time delay $\tau = 0.01$ s and $\tau = 0.1$ s with $\phi(x_k, t) = 5d \sin^3 \omega t$.

set because the "overlearning" results in oscillating when the sliding mode value is big. $G = 5.5 + 14\|\hat{\vartheta}_k^T(t)\psi(t)\|$ was set in order to guarantee the convergence because of the big control input time delay. Other parameters were not changed and the same as in this section.

The simulation results are shown in Figs. 18–20. The tracking errors are greater when the control input time delay is bigger, as shown in Fig. 18 in contrast with Fig. 14. The trajectory tracking effect is shown in Fig. 19, which becomes worsen. However, the ILC based on the IISM in this article still stabilizes it without chattering, and the control torques under different time delays are shown in Fig. 20.

## VIII. Application Example II

A three-tank system is a typical industrial process to be difficultly controlled, especially as liquid levels are coupled, nonlinear, and have a big inertia with input time delays.

Many researchers have studied its liquid-level control problem [41]–[45]. We used a vertical three-tank system to validate the proposed sliding mode ILC design, and the following approximate transfer function model was adopted to describe the liquid-level dynamic [44], [45]:

$$\frac{H_3(s)}{U(s)} = \frac{H_3(s)}{H_2(s)}\frac{H_2(s)}{H_1(s)}\frac{H_1(s)}{U(s)} = \frac{k_{p1}k_{p2}k_{p3}\, e^{-\tau s}}{(T_1 s+1)(T_2 s+1)(T_3 s+1)} \tag{46}$$

where $h_1(t)$, $h_2(t)$, $h_3(t)$, and $u(t)$ are the liquid levels of the first tank, second tank, third tank, and the pump control voltage, respectively, whose corresponding Laplace transformations are $H_1(s)$, $H_2(s)$, $H_3(s)$, and $U(s)$, respectively; $T_1$–$T_3$ are the time constants of the corresponding tanks; $k_{p1}$, $k_{p2}$, and $k_{p3}$ are the corresponding transmission gains; and $\tau$ is the time delay of the control input flow caused by the pipe.

Based on the transfer function description (46), the state-space model can be got as

$$\dot{h}(t) = Ah(t) + Bu(t-\tau)$$
$$A = \begin{bmatrix} -\frac{1}{T_1} & 0 & 0 \\ \frac{k_{p2}}{T_2} & -\frac{1}{T_2} & 0 \\ 0 & \frac{k_{p3}}{T_3} & -\frac{1}{T_3} \end{bmatrix}, \quad B = \begin{bmatrix} \frac{k_{p1}}{T_1} \\ 0 \\ 0 \end{bmatrix}$$

where $h(t) = [h_1(t), h_2(t), h_3(t)]^T$ is the level state vector. The state-space model can be transformed by

$$T = 10^3 \begin{bmatrix} 0 & 0 & 1 \\ 0 & \frac{k_{p3}}{T_3} & -\frac{1}{T_3} \\ \frac{k_{p2}k_{p3}}{T_2\ T_3} & -\frac{k_{p3}}{T_2\ T_3} - \frac{k_{p3}}{T_3^2} & \frac{1}{T_3^2} \end{bmatrix}, \quad z(t) = Th(t)$$

into the other state-space model

$$\dot{z}(t) = TAT^{-1}z(t) + TBu(t-\tau)$$

where $z(t) = [z_1(t), z_2(t), z_3(t)]^T$ is the transformed state vector. Substituting the matrices $T$, $A$, and $B$, we get

$$\begin{cases} \dot{z}_{k,1} = z_{k,2} \\ \dot{z}_{k,2} = z_{k,3} \\ \dot{z}_{k,3} = -\left[\frac{1}{T_1T_2T_3}, \frac{1}{T_1T_2} + \frac{1}{T_2T_3} + \frac{1}{T_1T_3}, \frac{1}{T_1} + \frac{1}{T_2} + \frac{1}{T_3}\right] z_k \\ \qquad\quad - \frac{k_{p1}k_{p2}k_{p3}}{T_1T_2T_3} \times 10^3\, u(t-\tau) \end{cases} \tag{47}$$

where $z_k = z_k(t) = [z_{k,1}(t), z_{k,2}(t), z_{k,3}(t)]^T$ is the state vector $z(t)$ along the iteration domain $k$.

For system (47), the sliding mode ILC control scheme was designed using the proposed IISM method, while the tracked curve was $y_d = 10^3\ h_{d,3}(t)$, with $h_{d,3}(t)$ being the aimed liquid level of the third tank. The control task was to make $h_3(t)$ tacking $h_{d,3}(t)$ with the tracking error $e_k(t) = [y_d - z_{k,1}, \dot{y}_d - z_{k,2}, \ddot{y}_d - z_{k,3}]^T$ converging. The parameters in (47) do not need to be known in the proposed method, but, in the application simulation, they were set as $T_1 = 72$, $T_2 = 34.4$, $T_3 = 23$, $k_{p1} = 0.26$, $k_{p2} = 1$, and $k_{p3} = 1$ referring to [44], [45]. The application simulation works were done as follows in the cases of $\tau = 0$ and $\tau \neq 0$.

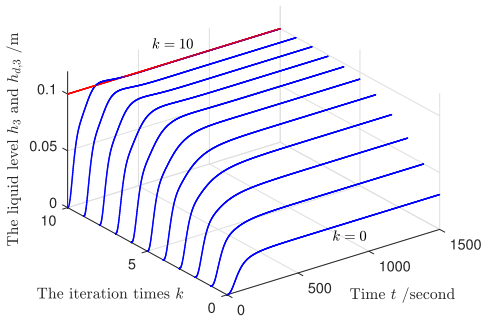


Fig. 21. Step responses $h_3(t)$ of the vertical three-tank system along with the iterations.

### A. Simulation Results When $\tau = 0$

First, the step signal $h_{d,3}(t) = 0.1$ was selected, and the following parameters were set in the IISM (4): $C^T = [1, 1, 1]$, $Q = 2$, $K^T = [0.88, 41, 101]$, $K_p^T = [0.02, 0.1, 1]$, $G = 0.001$, and $\varphi = 0.001$. For controller (13), $\xi(z_k, t) = z_k(t)$, $\beta_1 = 1 \times 10^{-6}$, and $\beta_2 = 0$ were selected for the update law (16). The response output $h_3(t)$ of the vertical three-tank system was observed under the step reference signal. Its responses along the iteration are shown in Fig. 21, and satisfactory transient performance is obtained only after ten iterations learning.

In contrast, we also applied the PID-SFCS control scheme in [45] to the vertical three-tank system, whose controller comprises a PID subcontroller and a state feedback subcontrol

$$U_{\text{PID}}(s) = \frac{0.042(49.9s+1)(49.4s+1)E_r(s)}{s(4.91s+1)}$$
$$u_{\text{SF}}(t) = -[2.55, 0.46, 0.03]h(t)$$

where $E_r(s)$ is the Laplace transform of the tracking error $e_r(t) = h_{d,3} - h_3(t)$. The step response output $h_3(t)$ was also observed and compared to that of the presented IISM method, as shown in Fig. 22. It can be seen that the transient response of the IISM method has the smaller overshoot, tuning time, and steady-state error.

To show the better tracking performance, the following reference signal was considered the target curve:

$$h_{3,d}(t) = \begin{cases} 0.12\sin\dfrac{\pi t}{2400}, & t \le 1200 \\ 0.03\sin\left(\dfrac{\pi t}{1200} - 0.5\pi\right) + 0.09, & t > 1200. \end{cases} \tag{48}$$

Except $\beta_1 = 3.5 \times 10^{-6}$, all the parameters had no change. Only after ten iterations of learning, its tracking outputs $h_3(t)$ along the iterations are shown in Fig. 23 and its sliding mode values in Fig. 24. In addition, the results of the IISM method were also compared with those of the PID-SFCS method, as shown in Fig. 25. The tracking output of the proposed IISM method has an obviously smaller steady-state tracking error.

*Remark 10:* The initial condition is $h_3(0) = h_{d,3}(0) = 0$, while the reference signal is the step signal $h_{d,3}(t) = 0.1$.

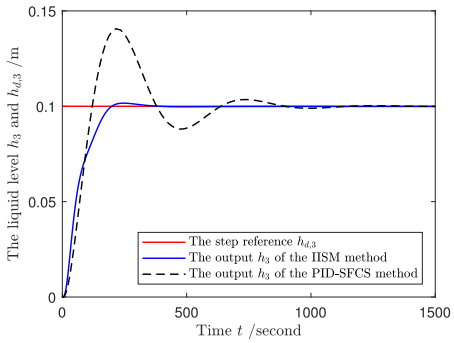


Fig. 22. Step responses $h_3(t)$ under the PID-SFCS and IISM methods.

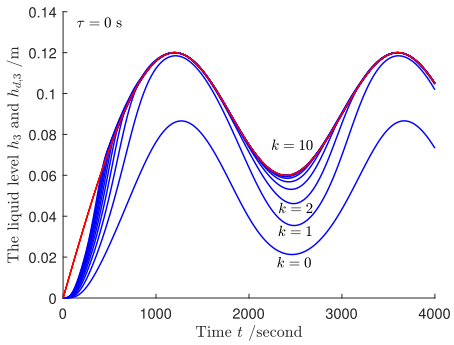


Fig. 23. Tracking responses $h_3(t)$ of the vertical three-tank system along with the iterations when $\tau = 0$.

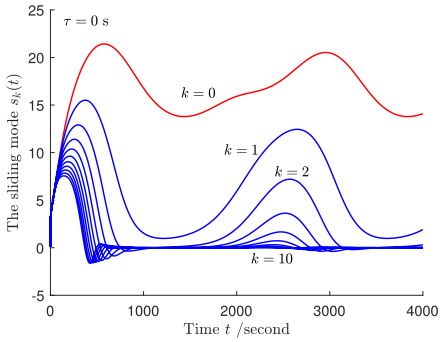


Fig. 24. Sliding mode value $s_k(t)$ along with the iterations when $\tau = 0$.

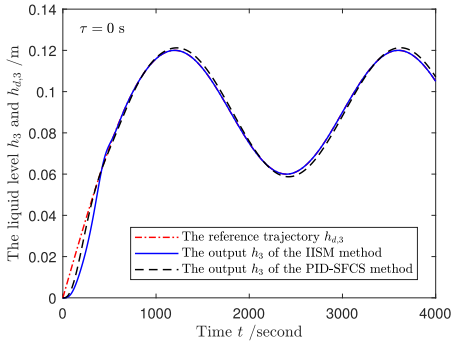


Fig. 25. Tracking responses $h_3(t)$ under the PID-SFCS and IISM methods when $\tau = 0$.

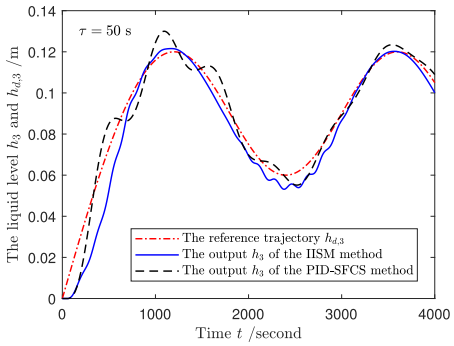


Fig. 26. Tracking responses $h_3(t)$ under the PID-SFCS and IISM methods when $\tau = 50$.

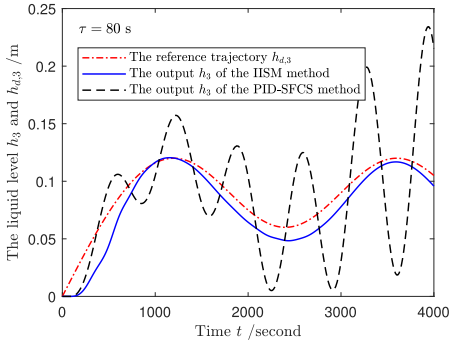


Fig. 27. Tracking responses $h_3(t)$ under the PID-SFCS and IISM methods when $\tau = 80$.

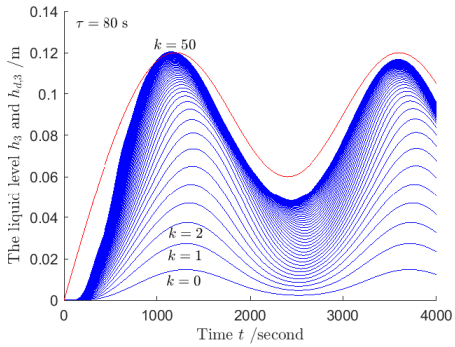


Fig. 28. Tracking responses $h_3(t)$ of the vertical three-tank system along with the iterations when $\tau = 80$.

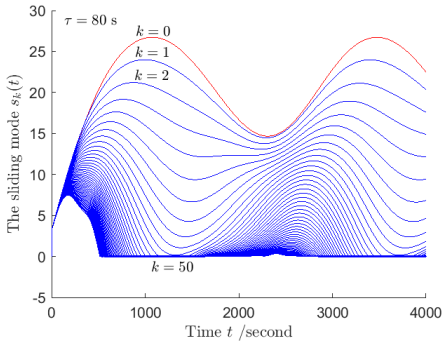


Fig. 29. Sliding mode value $s_k(t)$ along with the iterations when $\tau = 80$.

### *B. Simulation Results When $\tau \neq 0$*

Due to the length of the pipeline, there usually exists the input flow time delay. If the time delay is $\tau \neq 0$, the PID-SFCS scheme can still be used with a limited range of $\tau$. However, we would demonstrate that the proposed IISM method has a better tracking performance by overcoming the time delay.

First, we set $\tau = 50$, $K^T = [0.64, 81, 101]$, $\beta_1 = 8 \times 10^{-7}$, and $G = 0.001 + 12\|\hat{\vartheta}_k^T(t)\psi(t)\|$, and the other parameters had no change. After 30 iterations of learning, the tracking outputs

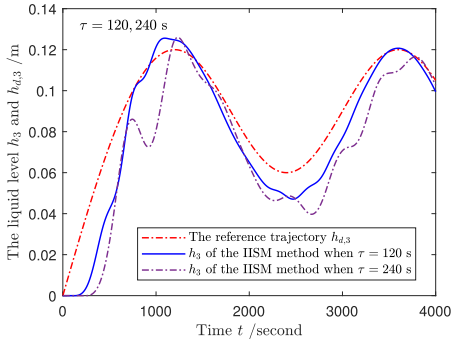


Fig. 30. Tracking responses $h_3(t)$ under the IISM methods when $\tau = 120$ and $\tau = 240$.

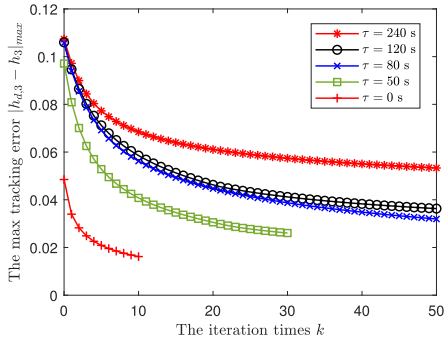


Fig. 31. Maximum tracking error $|h_{d,3} - h_3|_{\max}$ along with the iterations.

$h_3(t)$ of the PID-SFCS method and IISM method are shown in Fig. 26. Then, we set $\tau = 80$, $K^T = [0.52, 41, 81]$n and $G = 0.001 + 24\|\hat{\vartheta}_k^T(t)\psi(t)\|$, while the other parameters had no change. After 50 iterations of learning, the tracking outputs $h_3(t)$ are shown in Fig. 27. From the figure, the PID-SFCS scheme cannot stabilize the time-delay system dynamic when $\tau = 80$. On the contrary, the proposed IISM method is still effective. In this case, the tracking outputs $h_3(t)$ along the iterations are shown in Fig. 28, and its sliding mode values are shown in Fig. 29. In addition, $\tau = 120, 240$ were all set to verify the performance without any parameter change except $G = 0.001 + 36\|\hat{\vartheta}_k^T(t)\psi(t)\|$ as $\tau = 240$. The results are all shown in Fig. 30.

From Figs. 26, 27, and 30, it can be concluded that the tracking performance of the proposed IISM method is superior to that of the PID-SFCS method. Furthermore, the IISM method has the ability to stabilize the system with the unknown control input time delay without the requirements of knowing the exact parameters.

From Figs. 24 and 29, it can be seen that, by selecting the appropriate parameters, the value of the proposed IISM can be driven to zero along with the iterations. In addition, the tracking outputs in Figs. 23 and 28 get closer to the reference trajectory along with the sliding mode converging.

Fig. 31 shows the maximum tracking errors $|h_{d,3}(t) - h_3(t)|_{\max}$ along with the iteration $k$ under different time delays $\tau$. At a bigger time delay, the maximum tracking error converges to a greater value.

## IX. Conclusion

This article proposed an ILC control design based on the IISM surface to address the tracking problem of a class of nonlinear systems with unknown control input time delay. First, the IISM surface with iterative actions was proposed. The iterative actions in the IISM can reduce the tracking error without affecting the control design and convergence performance. The IISM also contains switching action to ensure reachability in both the time domain and the iteration domain. Then, the ILC controller was proposed based on the IISM. The update law of the controller is related to the IISM that promotes the sliding mode to converge to the origin in the iteration domain. The analytic results about the tracking stability under the controller were obtained. Finally, to overcome the chattering shortcoming of the SMC, measures were taken, and their influences on the tracking error were obtained through the analytic results. To verify our control design, the simulation applications on a one-link robotic manipulator and a vertical three-tank system were conducted. The results revealed that the IISM-based ILC has the capacity to stabilize the tracking from the initial iteration and the ability to overcome the unknown control input time delay.

## Acknowledgment

The authors thank the Editors and the Reviewers for their great works.

## References

[1] J.-X. Xu, S. K. Panda, and T. H. Lee, *Real-time Iterative Learning Control—Design and Application* (Advances in Industrial Control). London, U.K.: Springer-Verlag, 2009.
[2] D. A. Bristow, M. Tharayil, and A. G. Alleyne, "A survey of iterative learning control," *IEEE Control Syst. Mag.*, vol. 26, no. 3, pp. 96–114, Jun. 2006.
[3] R. W. Longman, "Iterative learning control and repetitive control for engineering practice," *Int. J. Control*, vol. 73, no. 10, pp. 930–954, Jan. 2000.
[4] T. Sugie and T. Ono, "Iterative learning control law for dynamical systems," *Automatica*, vol. 27, no. 4, pp. 729–732, 1991.
[5] R. Horowitz, W. Messner, and J. B. Moore, "Exponential convergence of a learning controller for robot manipulators," *IEEE Trans. Autom. Control*, vol. 36, no. 7, pp. 890–894, Jul. 1991.
[6] C.-J. Chien and J.-S. Liu, "P-type iterative learning controller for robust output tracking of nonlinear time-varying systems," *Int. J. Control*, vol. 64, no. 2, pp. 319–334, 1996.
[7] M. Sun and D. Wang, "Iterative learning control with initial rectifying action," *Automatica*, vol. 38, no. 7, pp. 1177–1182, Jul. 2002.
[8] J. Ghosh and B. Paden, "A pseudoinverse-based iterative learning control," *IEEE Trans. Autom. Control*, vol. 47, no. 5, pp. 831–837, May 2002.
[9] Y. Chen and C. Wen, *Iterative Learning Control: Convergence, Robustness, and Applications*. London, U.K.: Springer-Verlag, 1999.
[10] T.-J. Jang, H.-S. Ahn, and C.-H. Choi, "Iterative learning control for discrete-time nonlinear systems," *Int. J. Syst. Sci.*, vol. 25, no. 7, pp. 1179–1189, 1994.
[11] J.-X. Xu, "Analysis of iterative learning control for a class of nonlinear discrete-time systems," *Automatica*, vol. 33, no. 10, pp. 1905–1907, 1997.
[12] D. Wang, "Convergence and robustness of discrete time nonlinear systems with iterative learning control," *Automatica*, vol. 34, no. 10, pp. 1445–1448, 1998.
[13] C.-J. Chien, "A discrete iterative learning control for a class of nonlinear time-varying systems," *IEEE Trans. Autom. Control*, vol. 43, no. 5, pp. 748–758, May 1998.
[14] M. Sun and D. Wang, "Initial shift issues on discrete-time iterative learning control with system relative degree," *IEEE Trans. Autom. Control*, vol. 48, no. 1, pp. 144–148, Jan. 2003.
[15] J. Cai, R. Yu, B. Wang, C. Mei, and L. Shen, "Decentralized event-triggered control for interconnected systems with unknown disturbances," *J. Franklin Inst.*, vol. 357, no. 3, pp. 1494–1515, Feb. 2020.

[16] M. Zhang, P. Shi, L. Ma, J. Cai, and H. Su, "Quantized feedback control of fuzzy Markov jump systems," *IEEE Trans. Cybern.*, vol. 49, no. 9, pp. 3375–3384, Sep. 2019.
[17] H.-S. Ahn, Y. Chen, and K. L. Moore, "Iterative learning control: Brief survey and categorization," *IEEE Trans. Syst., Man, Cybern. C, Appl. Rev.*, vol. 37, no. 6, pp. 1099–1121, Nov. 2007.
[18] D. Shen, "Iterative learning control with incomplete information: A survey," *IEEE/CAA J. Automatica Sinica*, vol. 5, no. 5, pp. 885–901, Sep. 2018.
[19] D. Meng, Y. Jia, J. Du, and F. Yu, "Monotonically convergent iterative Learn. control for uncertain time-delay systems: An LMI approach," in *Proc. Amer. Control Conf.*, 2009, pp. 1622–1627.
[20] D. Meng, Y. Jia, J. Du, and F. Yu, "Robust iterative learning control design for uncertain time-delay systems based on a performance index," *IET Control Theory Appl.*, vol. 4, no. 5, pp. 759–772, May 2010.
[21] L. Wang, C. Zhu, J. Yu, L. Ping, R. Zhang, and F. Gao, "Fuzzy iterative learning control for batch processes with interval time-varying delays," *Ind. Eng. Chem. Res.*, vol. 56, no. 14, pp. 3993–4001, Apr. 2017.
[22] T. Liu, F. Gao, and Y. Wang, "IMC-based iterative learning control for batch processes with uncertain time delay," *J. Process Control*, vol. 20, no. 2, pp. 173–180, Feb. 2010.
[23] X. Dai, X. Tu, Y. Zhao, G. Tan, and X. Zhou, "Iterative learning control for MIMO parabolic partial difference systems with time delay," *Adv. Difference Equ.*, vol. 2018, no. 1, pp. 1–19, Dec. 2018.
[24] Y.-H. Lan and Y. Zhou, "D-type iterative learning control for fractional-order linear time-delay systems," *Asian J. Control*, vol. 15, no. 3, pp. 669–677, May 2013.
[25] Y.-H. Lan and Y. Zhou, "High-order-type iterative learning control for fractional-order nonlinear time-delay systems," *J. Optim. Theory Appl.*, vol. 156, no. 1, pp. 153–166, 2013.
[26] M. Lazarevic, N. Durovic, B. Cvetkovic, P. Mandic, and M. Cajic, "PD $\alpha$-type iterative learning control for fractional-order singular time-delay system," in *Proc. Chin. Control Decis. Conf.*, 2017, pp. 1905–1910.
[27] W. Chen and L. Zhang, "Adaptive iterative learning control for nonlinearly parameterized systems with unknown time-varying delays," *Int. J. Control, Autom. Syst.*, vol. 8, no. 2, pp. 177–186, Apr. 2010.
[28] L. Wang, S. Mo, D. Zhou, and F. Gao, "Robust design of feedback integrated with iterative learning control for batch processes with uncertainties and interval time-varying delays," *J. Process Control*, vol. 21, no. 7, pp. 987–996, Aug. 2011.
[29] J. Wei, Y. Zhang, M. Sun, and B. Geng, "Adaptive iterative learning control of a class of nonlinear time-delay systems with unknown backlash-like hysteresis input and control direction," *ISA Trans.*, vol. 70, pp. 79–92, Sep. 2017.
[30] D. Shen, Y. Mu, and G. Xiong, "Iterative learning control for non-linear systems with deadzone input and time delay in presence of measurement noise," *IET Control Theory Appl.*, vol. 5, no. 12, pp. 1418–1425, Aug. 2011.
[31] F. Ma, C. Li, and T. Huang, "Iterative learning control design of nonlinear multiple time-delay systems," *Appl. Math. Comput.*, vol. 218, no. 8, pp. 4333–4340, Dec. 2011.
[32] B. Xuhui, H. Zhanwei, H. Zhongsheng, and Y. Junqi, "Robust iterative learning control design for linear systems with time-varying delays and packet dropouts," *Adv. Difference Equ.*, vol. 2017, no. 1, pp. 1–17, Dec. 2017.
[33] Q. Yan, J. Cai, L. Wu, and Q. Zhou, "Error-tracking iterative learning control for nonlinearly parametric time-delay systems with initial state errors," *IEEE Access*, vol. 6, pp. 12167–12174, 2018.
[34] X.-D. Li, T. W. S. Chow, and J. K. L. Ho, "Iterative learning control for a class of nonlinear discrete-time systems with multiple input delays," *Int. J. Syst. Sci.*, vol. 39, no. 4, pp. 361–369, Apr. 2008.
[35] X.-D. Li, J. K. L. Ho, and M. Liu, "Robust iterative learning control with rectifying action for nonlinear discrete time-delayed systems," *Multidimensional Syst. Signal Process.*, vol. 25, no. 4, pp. 723–739, Oct. 2014.
[36] S. Hao, T. Liu, and W. Wang, "Robust output feedback based iterative learning control for batch processes with input delay subject to time-varying uncertainties," in *Proc. Chin. Control Decis. Conf. (CCDC)*, Yinchuan, China, May 2016, pp. 5790–5795.
[37] S. Hao, T. Liu, W. Paszke, and K. Galkowski, "Robust iterative learning control for batch processes with input delay subject to time-varying uncertainties," *IET Control Theory Appl.*, vol. 10, no. 15, pp. 1904–1915, Oct. 2016.
[38] J. K. Hale and S. M. V. Lunel, *Introduction to Functional Differential Equations*. New York, NY, USA: Springer-Verlag, 1993.
[39] Y. Xia and Y. Jia, "Robust sliding mode control for uncertain time-delay systems: A LMI approach," *IEEE Trans. Autom. Control*, vol. 48, no. 6, pp. 1086–1092, Aug. 2003.
[40] J. Ding and H. Yang, "Adaptive iterative learning control for a class of uncertain nonlinear systems with second-order sliding mode technique," *Circuits, Syst., Signal Process.*, vol. 33, no. 6, pp. 1783–1797, Jun. 2014.
[41] N. Orani, A. Pisano, and E. Usai, "Fault detection and reconstruction for a three-tank system via high-order sliding-mode observer," in *Proc. IEEE Int. Conf. Control Appl.*, Saint Petersburg, Russia, Jul. 2009, pp. 1714–1719.
[42] N. Orani, A. Pisano, and E. Usai, "Fault diagnosis for the vertical three-tank system via high-order sliding-mode observation," *J. Franklin Inst.*, vol. 347, no. 6, pp. 923–939, Aug. 2010.
[43] Z.-J. Yang and H. Sugiura, "Robust nonlinear control of a three-tank system using finite-time disturbance observers," *Control Eng. Pract.*, vol. 84, pp. 63–71, Mar. 2019.
[44] C.-A. Bojan-Dragos, A.-I. Szedlak-Stinean, R.-E. Precup, L. Gurgui, E.-L. Hedrea, and I.-C. Mituletu, "Control solutions for vertical three-tank systems," in *Proc. IEEE 12th Int. Symp. Appl. Comput. Intell. Informat. (SACI)*, Timisoara, Romania, May 2018, pp. 000593–000598.
[45] E.-L. Hedrea, R.-E. Precup, C.-A. Bojan-Dragos, C. Hedrea, D. Ples, and D. Popovici, "Cascade control solutions for level control of vertical three tank systems," in *Proc. IEEE 13th Int. Symp. Appl. Comput. Intell. Informat. (SACI)*, Timisoara, Romania, May 2019, pp. 352–357.

**Xiaoyu Zhang** (Senior Member, IEEE) was born in 1978. He received the B.S. degree from Yanshan University, Qinhuangdao, China, in 2000, and the M.S. and Ph.D. degrees from Zhejiang University, Hangzhou, China, in 2003 and 2006, respectively.

From June 2006 to June 2007, he taught at the School of Information Science and Engineering, Nanchang University, Nanchang, China. From 2007 to 2021, he taught at the North China Institute of Science and Technology, Langfang, China, and obtained the Associate Professor qualification in 2009 and the Professor qualification in 2016. From 2018 to 2019, he has been a Visiting Scholar at Columbia University, New York, NY, USA. In his research and teaching activities, he has been interested in nonlinear control, intelligent control, switching systems, driving systems, power electronics, and complex systems.

**Richard W. Longman** (Member, IEEE) has multiple degrees in aerospace, mathematics, and physics from the University of California at San Diego, San Diego, CA, USA, and the University of California at Riverside, Riverside, CA, USA.

He is a Professor of mechanical engineering and civil engineering at Columbia University, New York, NY, USA, was a Distinguished Romberg Guest Professor at Heidelberg University, Heidelberg, Germany, and had part-time positions at MIT, Bonn, Augsburg, National Cheng University, Newcastle Australia, and so on.

Dr. Longman is a fellow of AAS and AIAA. He served the AAS as a Vice President-Publications, a VP Technical, the First Vice President, and a member of the Board of Directors. He received the 50 000 Euro Award for lifetime achievement in research from the Alexander von Humboldt Foundation and the Dirk Brouwer Award from the American Astronautical Society (AAS) for contributions to spaceflight mechanics. He has given invited lectures at universities and government laboratories in 20 countries. He has many publications in iterative learning control, repetitive control, system identification, robotics in space, time optimal control, and so on.